Thermal and Spectroscopic Characterization of Microbial Poly(3-hydroxybutyrate) Submicrometer Fibers Prepared by Electrospinning

G.-M. Kim,[1] G. H. Michler,[1] S. Henning,[1] H.-J. Radusch,[2] A. Wutzler[2]

[1]*Department of Physics, Martin-Luther University Halle-Wittenberg, D-06099 Halle/S, Germany*
[2]*Department of Materials Science, Martin-Luther University Halle-Wittenberg, D-06099 Halle/S, Germany*

Received 19 July 2006; accepted 18 August 2006
DOI 10.1002/app.25348
Published online in Wiley InterScience (www.interscience.wiley.com).

ABSTRACT: Submicrometer fibers based on the microbially synthesized ultra-high-molecular-weight poly(3-hydroxybutyrate) (PHB) were generated by an electrospinning (ES) process with chloroform as the solvent. To characterize the resulting electrospun fibers in comparison with the pure PHB before ES, differential scanning calorimetry, Fourier transform infrared (FTIR) spectroscopy, scanning electron microscopy (SEM), and transmission electron microscopy were performed. The diameters of the electrospun fibers characterized by SEM were in the range 400–1000 nm. Thermal analysis showed that the electrospun fibers contained both helical (α form) and transzigzag (β form) crystals, whereas the solution-cast PHB films mostly possessed the common helical structure. In addition, the crystallinity of the electrospun PHB fibers increased compared to that of the solution-cast PHB films. Conformational changes occurred with the high extensional flow in the ES jets. Furthermore, the results from polarized FTIR measurements demonstrate that PHB molecules were oriented parallel to the fiber axis. As a result, the electrospun fibers exhibited strong birefringence under the polarized light. J Appl Polym Sci 103: 1860–1867, 2007

Key words: biofibers; differential scanning calorimetry (DSC); electron microscopy; FT-IR

INTRODUCTION

Poly(3-hydroxybutyrate) {[—$COCH_2CH(CH_3)O$—]$_n$; PHB} is a natural thermoplastic polyester that is produced by bacterial fermentation.[1–3] Because of its biodegradability without any toxic byproducts when disposed in a microbially active environment and its thermoplastic-like properties, similar to polypropylene, PHB has great potential as an environmentally friendly thermoplastic. In addition to those, due to its excellent biocompatibility with tissue and blood, PHB can be considered a polymer with potential in a variety of biomedical applications, such as biodegradable implant materials, drug-delivery vehicles, surgical dressing, stents, and tissue engineering scaffolds. However, its main shortcomings are its brittleness and thermal instability. It has been well established that PHB, in general, has a high tendency to crystallize due to its isotactic stereoregularity. Furthermore, the nucleation density of PHB is too low to initiate efficient crystallization. As a result, it forms spherulites of extremely large size, and thus, interspherulitic cracks are readily initiated within the large-size spherulites, which may be a cause of its brittleness.[4] Moreover, PHB is readily thermally degraded during processing, which leads to a narrow processing window.[5]

To overcome these shortcomings, tremendous efforts have been made to improve its mechanical performance and processibility in recent years, including (1) copolymerization with 3-hydroxyvalerate or 3-hydroxyhexanoate; (2) blending with other polymers such as poly(ethylene oxide),[6,7] poly(vinyl acetate),[8] and polyepichlorohydrin; and (3) the addition of a nucleating agent of either inorganic or organic molecules, such as talc, boron nitride,[9] and saccharin.[7] It is expected that the nucleation density will increase and the size of spherulites will decrease; thus, great improvement can be achieved in the elongation at break without the sacrifice of other desirable properties when tensilely loaded. Other physical methods have been also used to address these concerns; Furuhashi et al.[10] and Yamamoto et al.[11] succeeded in the melt-spinning and cold-drawing of poly(3-hydroxybutyrate-*co*-3-hydroxyvalerate) and reported its mechanical properties and detailed

This article is dedicated to F. J. Balta Calleja on the occasion of his 70th birthday.

Correspondence to: G.-M. Kim (gyeong.kim@physik.uni-halle.de).

Contract grant sponsor: Deutsche Forsungsgemeinschaft; contract grant number: SFB418 (to S.H.).

higher order structures. Gordeyev and Nekresov[12] reported oriented elastic PHB melt-spun fibers with high tensile strengths and moduli. More recently, Yamane et al.[13] reported that melt-spinning promoted the fraction of the β-zigzag form in PHB matrix, which occurred by the stretching of the amorphous tie molecules between lamellae. They demonstrated that an improvement in the mechanical properties of PHB fibers arose not only by the crystalline orientation of the α form but also by an increasing fraction of the β form.[13] In a previous work, we also found this kind of transition from the helical to the trans-zigzag conformation in electrospun PEO fibers.[14]

In this study, we attempted to use the electrospinning (ES) technique to fabricate polymer nanofibers on the basis of two hypotheses as follows. The first was that ES causes a strong shear force by the application of high electrostatic potential, which highly enforces the fluid jet ejection from the capillary to stretch the polymer molecules compared to conventional melt-spinning or cold-drawing. The other was that the resulting electrospun fibers are normally in submicrometer range; thus, such extreme confinements should be too small to build up large-size spherulites; that is, they should eliminate the formation of spherulites completely, which may prevent the growth of cracks responsible for material embrittlement. The objective of this research was, therefore, to study the effect of ES on the conformational changes of the resulting fibers, which could provide fundamental insights into the nature of the ES process.

EXPERIMENTAL

Materials and the ES process

PHB with an ultra-high-molecular-weight of about 900,000 g/mol and a polydispersity of 2.0 in chloroform solution was kindly supplied by the Center for Environmental Research (Leipzig-Halle, Germany). Before ES, the PHB solution was vigorously stirred with a magnetic stirring bar for at least 3 h at room temperature to ensure a homogeneous solution. ES was carried out under ambient temperature in a vertical spinning configuration with a flat-end needle with a 1-mm inner diameter and a 5-cm working distance. The applied voltages were in the range 3–20 kV and were driven by a high-voltage power supply (Knürr-Heizinger PNC, Resenheim, Germany). The electrospun fibers were collected either on transmission electron microscopy (TEM) copper grids or glass slides.

Electron microscopy

The preparation of samples for TEM was done as follows. At first, ultrathin PHB films were prepared by dip-coating of the mica substrates with a dilute solution of PHB in chloroform. After the evaporation of solvent, the films were placed on a hot stage for 2 min at 200°C and were subsequently crystallized for 6 h at 90°C in a vacuum oven. Afterward, the films were floated on water and transferred onto standard TEM copper grids. To study the semicrystalline morphology, we stained the ultrathin PHB films in RuO_4 vapor for 4 h and then examined them with a transmission electron microscope (Jeol 200CX, Tokyo, Japan) operating at an accelerating voltage of 200 kV. For analysis of the diameter of the electrospun fibers and their distribution, the electrospun fibers collected on the slide glasses were desiccated, directly sputter-coated with gold, and then examined with a field emission gun environmental scanning electron microscope (Philips ESEM XL 30 FEG, Eindhoven, The Netherlands) at an accelerating voltage of 5 kV.

Differential scanning calorimetry (DSC)

DSC measurements were conducted to measure the melting and crystallization behavior with a Mettler-Toledo DSC 820 (Giessen, Germany) under a nitrogen atmosphere. The samples were sealed in aluminum pans and were heated and cooled in the temperature range 25–200°C in the DSC instrument at a rate of 10 K/min. The weight of each sample was approximately 0.5 mg. The DSC temperature and heat flow values were calibrated with indium as a standard. For determination of the heat of fusion [or melting enthalpy (ΔH_m)] of the crystallized samples, these were heated to 200°C at a heating rate of 10 K/min. ΔH_m was calculated from the endothermal peak area from DSC.

Fourier transform infrared (FTIR) spectroscopy

An FTIR spectrometer (S2000, PerkinElmer) equipped with a fixed 100 μm-diameter aperture and a mercury–cadmium–telluride detector was used to analyze the absorbance in the wave number range 400–4000 cm^{-1} with a resolution of 2 cm^{-1}, with the conformational changes caused by the different processes monitored, that is, the solution casting and ES process of PHB. To identify the spectrum of amorphous PHB, the solution-cast PHB thin film was melted on the surface of a diamond crystal ATR (attenuated total reflection) cell (Golden Gate, Specac, Kent, UK) at 200°C. To characterize the PHB molecular orientation within the electrospun fibers, polarized FTIR measurements with a Zn–Se wire-grid IR polarizer were performed on two or three selected areas in a single electrospun fiber. At each area, the parallel and perpendicular spectra relative to the fiber axis were recorded.

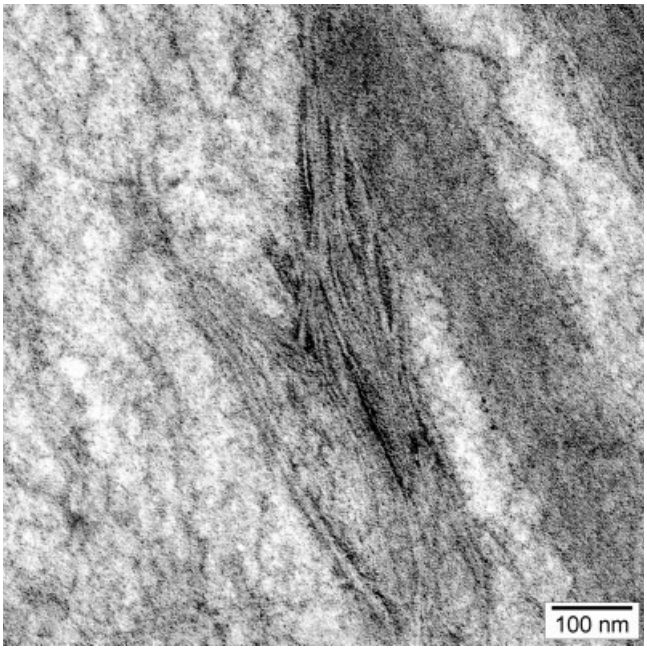

Figure 1 TEM micrograph of the phase morphology of the solution-cast PHB film.

RESULTS AND DISCUSSION

Morphology

Figure 1 shows a TEM micrograph of the solution-cast PHB film. One can clearly see the stacked lamellar morphology. The lamellar thickness was on the order of 6–13 nm. The most interesting observation was the lamellar orientation to a large extent, which was a part of lamellae within a spherulite. This observation was well consistent with results presented in the literature.[15,16]

A homogeneous PHB fibrous mat was produced by the ES process under the optimal fabrication parameters (10 kV, 5-cm working distance, and 1 mL/h feeding rate). Figure 2(a) shows a scanning electron microscopy (SEM) micrograph demonstrating that the 1 mm thick nanofibrous structure with three-dimensional polygonal pores was composed of randomly oriented nanofibers. The fiber diameter was in the range of 400–1000 nm, with an average fiber diameter of 700 nm [Fig. 2(b)]. Nanofibers deposited on the glass slides had good light transmission and exhibited birefringence under polarized light, which suggested anisotropic character of the electrospun fibers [Fig. 2(c)], which was caused by the arrangement of molecules or crystals parallel to the fiber axis during ES.

DSC

To investigate the thermal behavior, such as melting, crystallization, and the formation of crystalline structure, we performed DSC measurements. In the solution-cast PHB film, the single peak appeared both in endothermic and exothermic traces [melting peak = 170°C, crystallization temperature (T_c) = 62°C].[17] As known,

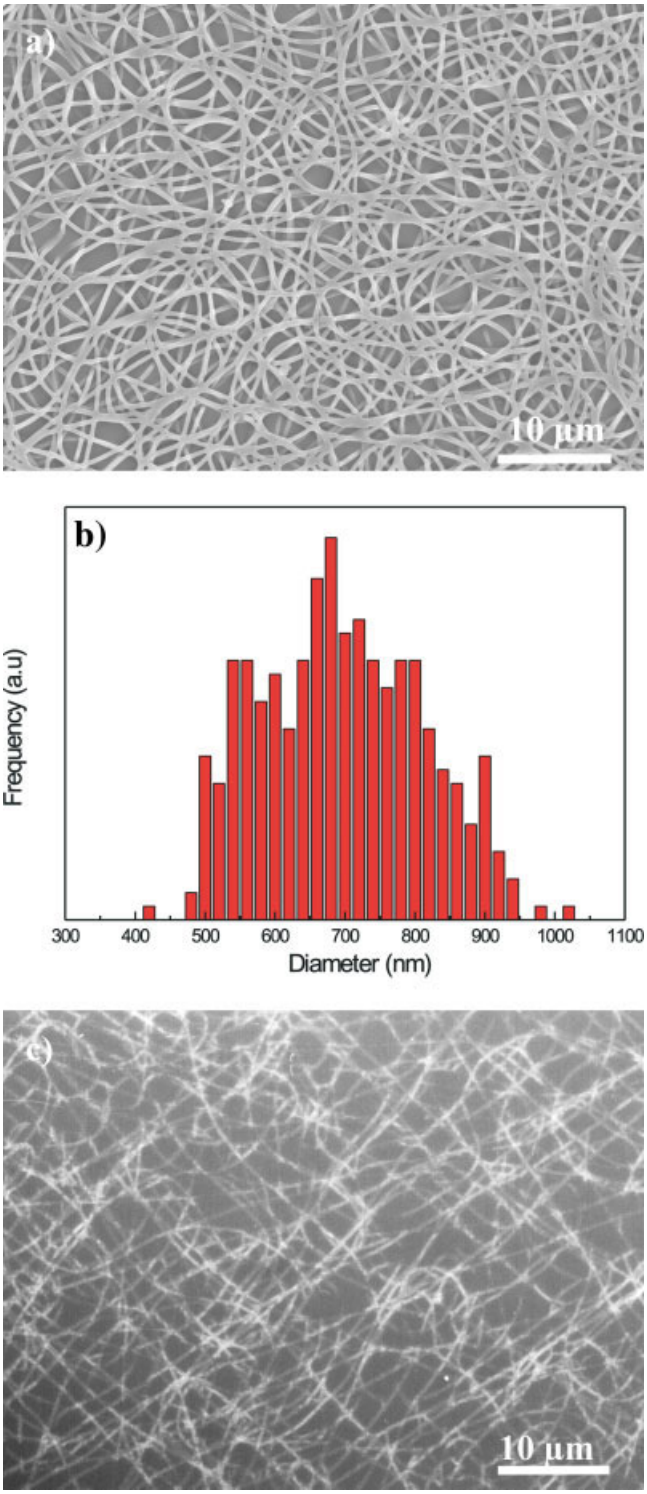

Figure 2 (a) SEM micrograph of electrospun PHB fibers on the glass substrate, (b) their diameter distribution, and (c) optical micrograph under polarized light. [Color figure can be viewed in the online issue, which is available at www.interscience.wiley.com.]

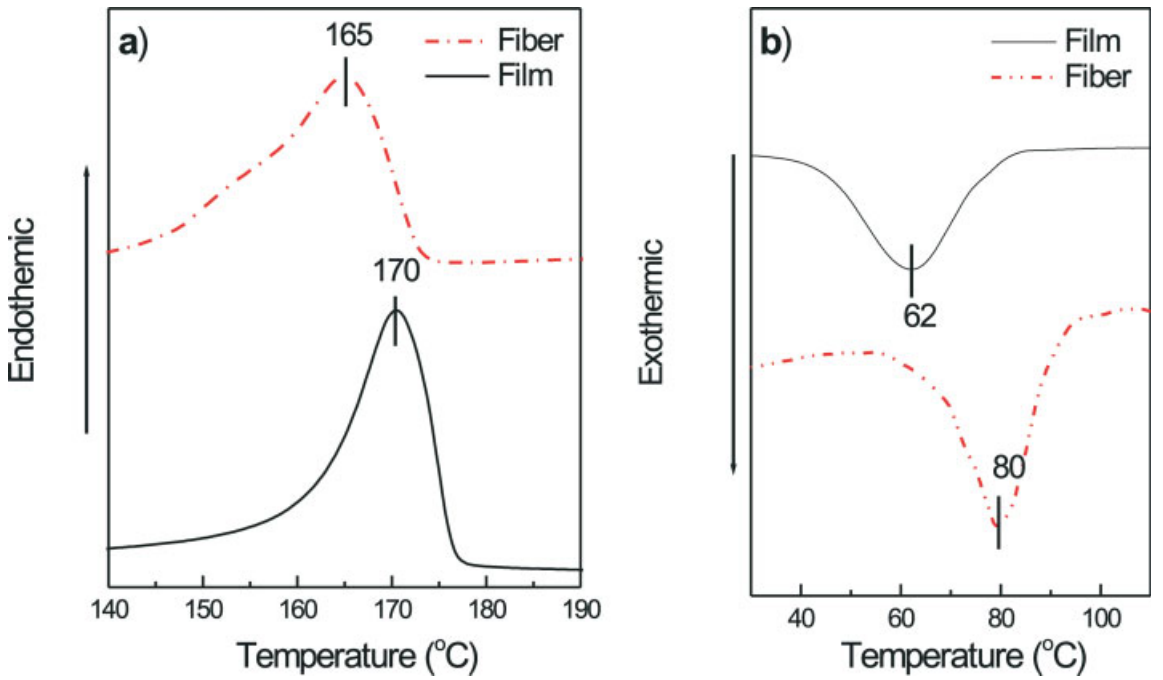

Figure 3 DSC diagrams for the solution-cast PHB film and electrospun PHB fibers: (a) endothermic and (b) exothermic traces. [Color figure can be viewed in the online issue, which is available at www.interscience.wiley.com.]

PHB can crystallize completely at a lower cooling rate; thus, a simple peak during the reheating process is a normal phenomenon for pure PHB. In contrast, the DSC measurement of the electrospun fibers showed that the melting peak shifted to a lower temperature at 165°C, whereas the crystallization peak shifted to a higher temperature at 80°C (Fig. 3).

It is well established that the transformation of helical macromolecules (the α form) to a planar zigzag conformation (the β form) occurs in conventional semicrystalline systems when they stretched and/or cold-drawn[18–20] and in electrospun semicrystalline fibers, as shown by our previous results.[14] The formation of the β form induced by cold-drawing in PHB was demonstrated by Orts et al.,[21] who suggested that the β form chains emanated on stretching from the amorphous domains between orthorhombic α-form lamellae. They showed from DSC measurements and wide-angle X-ray scattering studies that the β form is produced during drawing and annealing processes and is rather more disordered than the α form.[13]

On the analogy of the cold-drawing, the strong shear forces in the ES jet may cause the breakage of the long chains of the crystalline complex into small parts. The structure of the solution-cast PHB film, which mainly consisted of the helical chains (the α form), would be transformed into the extended-chain conformation (the β form), which form was generated by the stress-induced crystallization of the quasi-amorphous interlamellar phase in the PHB matrix during the ES process. As a result, the electrospun PHB fibers revealed a coexisting morphology composed of both α and β crystalline forms. Moreover, the overall crystallinity (X_c; associated with ΔH_m) of electrospun fibers increased compared to that of the cast film. When the electrospun fibers were being reheated, the double peak appeared in the endothermic trace; the β form crystals were first melted at a lower temperature, and then, the α form was melted at a higher temperature, which was attributed to α crystals that were the same as in the cast PHB film. Conversely, during the cooling process, the β form crystals crystallized before the occurrence of an intense endothermic peak by the α form.

The DSC data for the PHB film and electrospun PHB fibers are listed in Table I. In general, the melting temperature (T_m) and T_c are considered indirect measures of X_c and the crystallization rate. The main T_c value of the cast PHB film shifted to a higher temperature ($\Delta T_c = 18$°C) and its peak area became narrower on ES, which indicated that the ES procedure significantly promoted the crystallization

TABLE I
T_m, T_c, ΔH_m, and Calculated X_c

	T_m (°C)	T_c (°C)	ΔH_m (J/g)	X_c (%)
Cast film	170	62	68.52	47
ES fibers	165	80	73.44	50

rate of PHB, corresponding to the rapid crystallization. This result may be at least in part attributed to the confinement of electrospun fibers, which was provided by high degree of supercooling during the ES process, which led to the rapid formation of heterogeneous crystallization nuclei compared to the cast PHB film. As reported in Table I, from the enthalpy associated with the melting endotherm, X_c of the samples studied was calculated by eq. (1):

$$X_c = \frac{\Delta H_m}{\Delta H_{mo}} \quad (1)$$

where ΔH_m is the area of the melting peaks and ΔH_{mo} (the heat of fusion of 100% crystalline PHB) = 146 J/g, as taken from the literature.[22] After the ES procedure, T_m shifted to a lower value compared with that of the cast PHB film. However, ΔH_m (and X_c) increased moderately after ES. This indicated that the ES procedure favored an increase in the overall X_c of PHB.

This was attributed to further crystallization due to improved mobility of the molecules because the new PHB film was heated immediately after complete evaporation of the solvent and was not yet completely crystallized. When the sample was heated to 160°C, the absorbance of the crystalline and the amorphous bands showed abrupt changes until the sample was completed melted at 180°C. These changes agreed well with the DSC results, as shown in Figure 3. From the spectrum, during heating of the newly cast PHB film, there existed a sharp endotherm, and the lamellae were mostly melted between 160 and 180°C, with the maximum melting rate at 175.5°C.

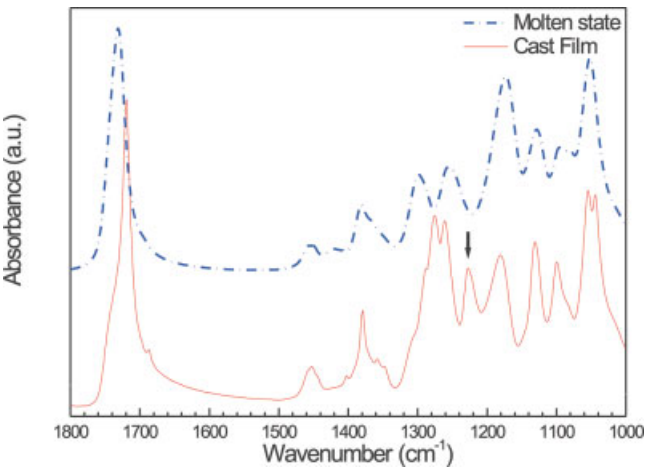

Figure 4 FTIR spectra for the molten state of solution-cast PHB and the electrospun PHB fibers. [Color figure can be viewed in the online issue, which is available at www.interscience.wiley.com.]

FTIR spectroscopy

Although DSC is informative for thermal behavior, it does not give any information about the nature of the conformational changes from the ES procedure. Because FTIR is sensitive to the local molecular environment, we performed FTIR measurements to characterize the conformational changes in the PHB matrix on ES. At first, to get better insight into the special differences between amorphous and crystalline PHB, we heated a sample of the solution-cast PHB film on an ATR cell over its T_m at 200°C and recorded absorption spectra. The spectra observed are shown in Figure 4, and the absorption peaks and their assignments are summarized in Table II.[23–26]

TABLE II
FTIR Absorption Peaks for Amorphous and Crystalline PHB Films and Electrospun PHB Fibers with Their Assignments

Absorption peak			
Amorphous PHB film	Crystalline PHB film	Electrospun PHB fiber	Assignment
	2934		Methylene C—H
1731			C—O stretching
		1723	C=O stretching amorphous carbonyl group
	1719		C=O stretching crystalline carbonyl group
1453			C—H bending
	1452	1452	Asymmetric CH_3
1380	1379	1379	Symmetric CH_3
1299			C—O—C stretching
	1275		Asymmetric C—O—C stretching
1255	1261	1261	Symmetric C—O—C stretching
	1227	1227	CH_3 vibration
	1180	1180	Asymmetric C—O—C stretching
1173			C—O stretching
1128	1130	1130	Asymmetric C—O stretching
1096	1099	1099	Symmetric C—O stretching
1052	1054	1056	C—O stretching and CH_2 rocking
	1044	1044	C—O stretching and CH bending

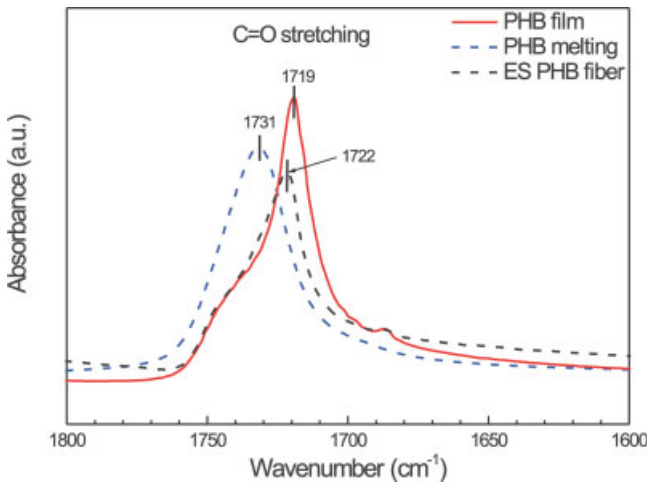

Figure 5 FTIR spectra for the (a) C=O stretching regime and (b) C—H bending and C—O—C and C—O stretching regime. [Color figure can be viewed in the online issue, which is available at www.interscience.wiley.com.]

In comparison, the FTIR spectrum of purely amorphous PHB was obtained from the molten state of PHB, and the peaks were at 1731, 1453, 1380, 1299, 1255, 1173, 1128, 1096, and 1052 cm^{-1}. These singlet bands were attributed to the vibrational modes of conformationally irregular PHB chains (purely amorphous). A striking difference seen in the spectra was the band at 1227 cm^{-1}, which was visible for the crystalline PHB phase and disappeared completely in the molten state (arrow in Fig. 4).

To analyze the FTIR spectra in more detail, we divided it into two spectral regions: one was 1700–1760 for C=O stretching, and the other was 1400–1000 for C—H bending and C—O—C and C—O stretching. Figure 5 shows the spectra of the cast PHB film and its melting and the electrospun PHB fibers in the C=O stretching regime. The C=O stretching vibration at 1719 cm^{-1} shifted to 1731 cm^{-1} on solution casting and ES of PHB. It is well established that the band observed at 1731 cm^{-1} is due to the amorphous phase, whereas the band at 1719 cm^{-1} was assigned to the highly ordered crystalline structure.[27]

The shift of spectral bands to the higher values may have been closely associated with the altered local orientation distribution of electric dipole-transition moments caused by the melting and ES of PHB. During melting, the mobility of molecules increased, and the oxygen atoms of the carboxyl groups loosened to the hydrogen atoms at the other segments; thus, the increased dipole moments resulted in a higher wave number of the band. The shift caused by the ES could not simply be explained by the changing of dipole moments because the confinement of the fiber normally induces closer packing of PHB molecules, which results in the reduction of dipole moment, that is, a decreasing wave number. The minor increase in the wave number on ES could be explained only by the conformational changes resulting from the strong shear forces in the ES. In previous work, we showed that the transition of helical macromolecules to a planar zigzag conformation occurred in electrospun PEO fibers. Recently, it was well established that PHB also shows a strain-induced transition from the α form to the β form, of which the β form is an energy-minimized conformation.[13] In general, the PHB crystallizes via a helical conformation, where the methyl groups have a low volume and high spatial symmetry. Consequently, they could easily pack together to form α crystals. After that, the closely packed chains turned into trans-zigzag conformers during the ES process.

Figure 6(a) shows the bands in the range 1400–1000 cm^{-1}. It is clear that the bands at 1381, 1128, 1096, and 1052 cm^{-1}, which arose from the amor-

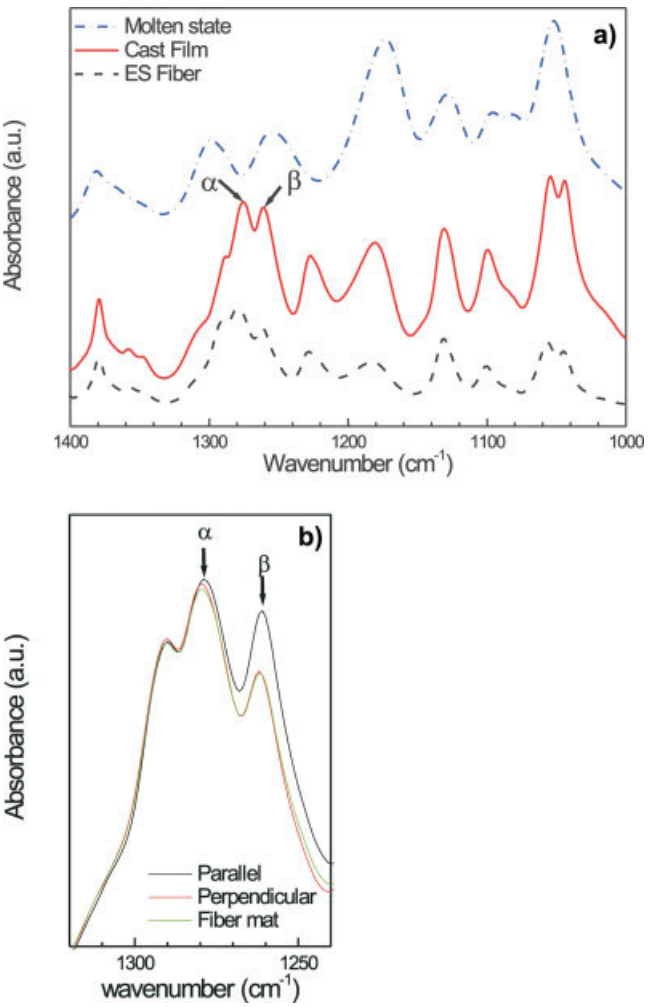

Figure 6 FTIR spectra for the (a) molten state of PHB, the solution-cast PHB, and the electrospun PHB fibers and (b) selective α and β crystal peaks from the polarized FTIR measurements. [Color figure can be viewed in the online issue, which is available at www.interscience.wiley.com.]

TABLE III
Absorbance Peaks for the α and β Crystal Forms, Relative Population Ratios, and Fractions of the α-to-β Transformation

	α (A_{1275})	β (A_{1261})	α/β ratio	α/β (%)
Cast PHB film	337	323	1.04	
ES PHB fiber	275	226	1.22	17

phous phase of PHB, still existed with minor shifting of the wave number in both spectra of the cast film and electrospun fibers. In the spectra of crystalline PHB from the cast film and electrospun fiber, the bands at 1275, 1261, 1227, 1180, 1054, and 1044 cm^{-1} were distinctly present, although they were not present in the spectrum of amorphous PHB. Interestingly, the bands from the electrospun fibers were identical to the solution-cast PHB; except for variations in the intensity of these bands, all peaks remained at the same location; that is, no significant shifts were visible. These results strongly suggest that they were in the semicrystalline state.

To obtain deeper insight into the α and β populations, we selectively considered the ratio between 1275 and 1261 cm^{-1} [arrows in Fig. 6(b)], respectively.[28] The reason is based on the results from several authors who identified the intensity of band at 1275 cm^{-1} as the highly ordered helix conformation. Other strong lines were more or less in correspondence with the two conformational modifications and, therefore, were not taken into account. As shown in Table III, the α/β absorbance ratio (i.e., A_{1275}/A_{1261}) increased after ES, which indicated an increase in the β population, which may have occurred by the stretching of the amorphous tie molecules between PHB lamellae. The degree of the α-to-β conformational transformation of PHB on ES could be calculated as follows

$$\alpha\beta(\%) = \left[\frac{(A_{1275}/A_{1261})_{\text{fiber}}}{(A_{1275}/A_{1261})_{\text{film}}} - 1\right] \times 100\% \qquad (2)$$

The α/β ratio was 17%, which indicated that the strong shear forces caused by ES facilitated the PHB chains to be preferentially more aligned in the fiber direction. The electrospun PHB fibers, therefore, involved the highly ordered crystalline component and consisted of both the α and β form coupled with the amorphous structure. These results were well consistent with those observed from PHB under simple tension or conventional cold-drawing.[29]

To characterize the degree of molecular orientation of PHB within the electrospun fibers, polarized FTIR measurements were performed. The results are shown in Figure 6(b), where the most characteristic β band at 1261 cm^{-1} was taken into consideration. Analysis was carried out by calculation of the dichroic ratio (R) as the degree of molecule orientation, defined as follows:

$$R = A_{1261\parallel}/A_{1261\perp} \qquad (3)$$

where the subscripts ∥ and ⊥ denote the parallel and perpendicular orientations relative to the fiber axis, respectively. The observed R value was 1.14 for the electrospun PHB fibers [Fig. 6(b)]. This indicated that the PHB molecules in the electrospun fibers were more preferentially oriented parallel to the fiber axis than in the cast film.

CONCLUSIONS

In this study, the ES process was attempted to fabricate polymer nanofibers based on microbially synthesized PHB, of which the average diameter was about 700 nm. The electrospun PHB fibers were uniform but randomly oriented in the resulting nonwoven fiber mats. Melting and crystallization of the solution-cast PHB film and electrospun fibers were studied via FTIR combined with DSC. Distinct amorphous bands were found at 1731, 1299, 1255, and 1173 cm^{-1}, and the bands at 1719, 1275 1261, 1227, and 1180 cm^{-1} were considered characteristic for crystalline peaks. Some bands among the amorphous peaks in the FTIR spectra were still contained in the solution-cast film and in the electrospun fibers. These results were consistent with those from DSC. It was demonstrated that the ES promoted an increase in X_c of PHB and facilitated the formation of β crystals from the amorphous tie molecules between the lamellae. Polarized FTIR spectrum of the electrospun PHB fiber indicated that the PHB molecules were more highly aligned in the fiber direction, which was caused by the strong shear forces in the ES procedure. Finally, we concluded that the electrospun fibers had a complex morphology composed of the α and β forms and the amorphous component.

The authors thank UFZ-Umweltforschungszentrum Leipzig-Halle GmbH for supplying the PHB.

References

1. Doi, Y. Microbial Polyesters; VCH: New York, 1990.
2. Hasirci, V. In Biomaterials and Bioengineering Handbook; Wise, D. L., Ed.; Marcel Dekker: New York, 2000; p 141.
3. Lee, S. Y. Biotechnol Bioeng 1996, 49, 1.
4. El-Hadi, A.; Schnabel, R.; Straube, E.; Müller, G.; Riemschneider, M. Macromol Mater Eng 2002, 287, 363.
5. Weihua, K.; He, Y.; Asakawa, N.; Inoue, Y. J Appl Polym Sci 2004, 94, 2466.
6. Avella, M.; Greco, P.; Martuscelli, E. Polymer 1991, 32, 1647.

7. Avella, M.; Martuscelli, E.; Raimo, M. Polymer 1993, 34, 3234.
8. Greco, P.; Martuscelli, E. Polymer 1989, 30, 1475.
9. Withey, R. E.; Hay, J. N. Polymer 1999, 40, 5147.
10. Furuhashi, Y.; Ito, H.; Kikutani, T.; Yamamoto, T.; Kimizu, M.; Cakmak, M. J Polym Sci Part B: Polym Phys 1998, 36, 2471.
11. Yamamoto, T.; Kimizu, M.; Kikutani, T.; Furuhashi, Y.; Cakmak, M. Int Polym Process 1997, 12, 29.
12. Gordeyev, S. A.; Nekrasov, Y. U. P. J Mater Sci Lett 1999, 18, 1691.
13. Yamane, H.; Terao, K.; Hiki, S.; Kimura, Y. Polymer 2001, 42, 3241.
14. Kim, G.-M.; Wutzler, A.; Radusch, H.-J.; Michler, G. H.; Simon, P.; Sperling, R. A.; Parak, W. J. Chem Mater 2005, 17, 4949.
15. Abe, H.; Doi, Y.; Akehata, T. Macromolecules 1998, 31, 1791.
16. Abe, H.; Kikkawa, Y.; Iwata, T.; Aoki, H.; Akehata, T.; Doi, Y. Polymer 2000, 41, 867.
17. Buckley, C. P.; Kovacs, A. J. In Structure of Crystalline Polymers; Hall, I. H., Ed.; Elsevier Applied Science: London, 1984.
18. Prud'homme, R. E.; Marchessault, R. H. Macromolecules 1974, 7, 541.
19. Feughelman, M. J. J Appl Polym Sci 1966, 10, 1937.
20. Fraser, R. D. B.; MacRae, T. P. Conformation in Fibrous Proteins and Related Synthetic Polypeptides; Academic: New York, 1973; p 179.
21. Orts, W. J.; Bluhm, T. L.; Hamer, G. K.; Marchessault, R. H. Macromolecules 1990, 23, 26.
22. Barham, P. J.; Keller, A.; Otun, E. L.; Holmes, P. A. J Mater Sci 1984, 19, 2781.
23. Manna, A.; Imae, T.; Yogo, T.; Aoi, K.; Okazaki, M. J Colloid Interface Sci 2002, 256, 297.
24. Porter, M. D.; Bright, T. B.; Allara, D. L.; Chidsey, C. E. D. J Am Chem Soc 1987, 109, 3559.
25. Lambeek, G.; Vorenkamp, E. J.; Schouten, A. J. Macromolecules 1995, 28, 2023.
26. Marentrtte, J. M.; Brown, G. R. Polymer 1998, 39, 1405.
27. Padermshoke, A.; Katsumoto, Y.; Sato, H.; Ekgasit, S.; Nodad, I.; Ozaki, Y. Polymer 2004, 45, 6547.
28. Shieh, Y. T.; Liu, K. H. J Polym Sci Part B: Polym Phys 2004, 42, 2479.
29. Furuhashi, Y.; Ito, H.; Kikutani, T.; Yamamoto, T.; Kimizu, M.; Cakmak, M. J Polym Sci Part B: Polym Phys 1998, 36, 2471.